CRYSTAL GROWTH & DESIGN

Article

pubs.acs.org/crystal

Guest–Host Frameworks of the Anionic Metal Complex $[Fe(ox)_3]^{3-}$ and Cationic Bipyridinium-Based Linkers Bonded by Charge-Assisted Hydrogen Bonds

M. Jaya Prakash, Allen G. Oliver, and Slavi C. Sevov*

Department of Chemistry and Biochemistry, University of Notre Dame, Notre Dame, Indiana 46556, United States

Supporting Information

ABSTRACT: Reported is the synthesis and characterization of guest-free and guest-included frameworks assembled from the anionic metal complex $[Fe(ox)_3]^{3-}$ and the cationic diprotonated 4,4′-bipyridinium^{2+} (H_2bpy) or 1,2-bis(4-pyridinium)ethylene^{2+} (H_2bpye) linkers, where the complex and linkers are bonded by multiple charge-assisted hydrogen bonds. In some of the compounds additional barium cations serve as bridges between the anionic metal complexes forming $-\{[Fe(ox)_3^{3-}]_2[Ba^{2+}]\}_\infty-$ anionic infinite chains. Aromatic guest molecules of 4-methoxyphenol (mp), 1,6-dimethoxynaphtalene (dmn), and 1,5-dihydroxynaphthalene (dhn) were successfully incorporated in the cavities of the frameworks. The $\pi-\pi$ interactions between the pillars and the guests in the resulting guest-included frameworks were confirmed spectroscopically. The magnetic properties of the frameworks were measured as well.

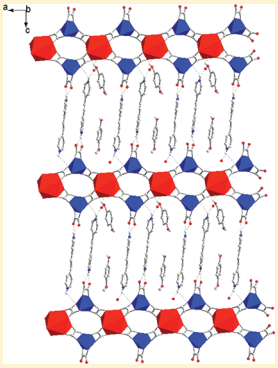

INTRODUCTION

The host–guest inclusion compounds are a class of flexible (or soft) frameworks capable of hosting diverse guest molecules by adjusting bonding modes (angles, distances, etc.) and/or molecular conformations in order to create appropriate cavities for the guest. At the same time, these adjustments are such that the basic framework connectivity remains largely unchanged.[1] All this makes such compounds interesting not only from a synthetic point of view but also as potential materials for catalysis, separation, and molecular recognition.[2]

One particular class of soft frameworks are those built of cations and anions that are held together by multiple charge-assisted hydrogen bonds. The combination of electrostatic interactions and hydrogen bonds strengthens the framework and provides additional stability.[1,3] The typical design of such framework is based on cationic nodes, either organic molecules or metal complexes, that are connected by anionic organic linkers such as disulfonates. It has been shown by Ward et al. that such frameworks made of guanidinium cations and different disulfonate anions can accommodate a large variety of guest molecules.[1,4] Later, the guanidinium cations were "replaced" by cationic metal complexes with ligands capable of similar hydrogen bonding such as amines, ammonia, and water.[5,6] The potential advantage of this replacement is eventual redox capabilities as well as valuable magnetic properties of the resulting compounds. In addition to the frameworks with cationic nodes and anionic linkers, there is also a growing number of frameworks with reversed polarity, i.e., with anionic metal complexes and cationic linkers, that exhibit the same charge-assisted hydrogen bonding.[7]

One of the problems encountered early with using metal complexes was their typically high positive charge, e.g., $[M^{III}L_6]^{3+}$, where L is a neutral ligand. This, when combined with the lower negative charge of −2 for the disulfonate linkers, resulted in a high number of linkers per cation, 1.5, and thus smaller cavities. This was resolved in two different ways. One of them used modified metal complex with some anionic ligands and lower charge such as $[Co(en)_2(ox)]^+$, for example.[5a,b] The second approach was to include small "spectator" anions such as Cl^- in $[Co(NH_3)_6][PIPES]Cl{\cdot}6H_2O$ (PIPES = 1,4-piperazinebisethanesulfonate) that do not occupy valuable space and yet effectively reduce the positive charge.[6] Both approaches result in the need of only one dianionic sulfonate pillar per node instead of otherwise one and a half. This, in turn, leaves larger interpillar galleries in the structure. These solutions to high charge issues are, of course, applicable to reversed charge systems. Thus, we recently reported host–guest frameworks made of the monoanionic metal complex $[Co(en)(ox)_2]^-$ and diprotonated bipyridinium dications, i.e., $[Co(en)(ox)_2]_2[H_2bpy]{\cdot}n(guest)$.[8] The charge of this complex is already reduced compared to $[Co(ox)_3]^{3-}$ in a similar way by replacing an anionic ligand with a neutral one. Continuing this work, we wanted to apply the second approach for "lowering" the charge of the homoleptic metal complexes $[M(ox)_3]^{3-}$ by introducing a small spectator cation. This was accomplished by incorporating Ba^{2+} cations in the here reported frameworks made of $[Fe(ox)_3]^{3-}$ nodes and 4,4′-bipyridinium^{2+} (H_2bpy) or

Received: February 29, 2012
Revised: April 2, 2012
Published: April 5, 2012

1,2-bis(4-pyridinium)ethylene^{2+} (H_2bpye) linkers and hosting 4-methoxyphenol (mp), 1,6-dimethoxynaphthalene (dmn), and 1,5-dihydroxynaphthalene (dhn) as guest molecules (Chart 1).

Chart 1. Linkers and Guest Molecules

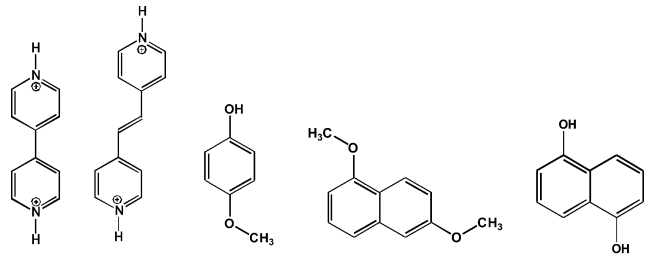

EXPERIMENTAL SECTION

$K_3[Fe(ox)_3]\cdot 3H_2O$ was synthesized according to the literature.[9] 4,4′-Bipyridine (bpy, Sigma Aldrich), 1,2-di(4-pyridyl)ethylene (bpye, Sigma Aldrich), 4-methoxyphenol (Alfa-Aesar), 1,6-dimethoxynaphthalene (Alfa-Aesar), 1,5-dihydroxynaphthalene (TCI), and methanol (Fischer Scientific) were used as received without further purification. FT-IR spectra of the freshly prepared compounds in crystalline form were recorded on a Bruker TENSOR-27 FT-IR spectrophotometer in ATR mode in the 4000−400 cm^{-1} region. UV−vis spectra were recorded for solid samples on JASCO V-670 machine in reflectance mode in the 200−900 nm region.

Synthesis of $[H_2bpy][Hbpy][Fe(ox)_3]\cdot 2.5H_2O$ (1). A solution of $K_3[Fe(ox)_3]\cdot 3H_2O$ (0.41 mmol) in 20 mL of water was mixed with 20 mL of an aqueous solution of 4,4′-bipyridinium dichloride (H_2bpyCl_2) (0.8 mmol) and the mixture was left undisturbed at room temperature to allow for slow evaporation. Light green colored block-shaped crystals of **1** were obtained in 2 days as a single phase. Yield = 85%. IR (cm^{-1}): 1641, 1708, $\nu_{C=O}$, oxalate; 1604, 1384, $\nu_{C=C}$, 1486, $\nu_{C=N}$, 3510, ν_{N-H}, H_2bpy. Anal. Calcd for $C_{52}H_{48}N_8O_{29}Fe_2$: C, 45.9; H, 3.56; N, 8.24. Found: C, 44.21; H, 3.48; N, 8.02.

Synthesis of $[H_2bpye][Hbpye][Fe(ox)_3]_{0.88}[Fe_2(ox)_5]_{0.12}\cdot 2H_2O$ (2). A solution of $K_3[Fe(ox)_3]\cdot 3H_2O$ (0.5 mmol) in 20 mL of water was mixed with 20 mL of aqueous solution of 1,2-di(4-pyridinium)-ethylene dichloride ($H_2bpyeCl_2$) (0.8 mmol) and left undisturbed at room temperature to allow for slow evaporation. Light green block-shaped crystals of **2** were obtained in 2 days as a single phase. Yield = 80%. IR (cm^{-1}): 1660 (s), 1706 (m), $\nu_{C=O}$, oxalate; 1625 (m), 1377 (m), $\nu_{C=C}$, 1504 (s), $\nu_{C=N}$, 3513 (m), ν_{N-H}, H_2bpye. Anal. Calcd for $C_{59.77}H_{54}N_8O_{27.54}Fe_2$: C, 49.97; H, 3.79; N, 7.80. Found: C, 48.77; H, 3.53; N, 7.64.

Synthesis of $Ba[H_2bpye]_2[Fe(ox)_3]_2\cdot 1.5(mp)\cdot 4.5H_2O$(3). Twenty milliliters of aqueous solutions of $K_3[Fe(ox)_3]\cdot 3H_2O$ (0.8 mmol) and $H_2bpyeCl_2$ (0.8 mmol) were mixed with 5 mL of methanol solutions of 4-methoxyphenol (mp) (1.5 mmol) and $BaCl_2$ (1.0 mmol) and were then left undisturbed at room temperature to allow for slow evaporation. Dark-red, block-shaped crystals of **3** were obtained in 10 days as a single phase. Yield = 92%. IR (cm^{-1}): 1651, 1707, $\nu_{C=O}$, oxalate; 1230, ν_{C-O}, mp; 1624, 1392, $\nu_{C=C}$, 1504, $\nu_{C=N}$, 3420, ν_{N-H}, H_2bpye. Anal. Calcd for $C_{372.8}H_{352}N_{32}O_{251.2}Fe_{16}Ba_8$: C, 39.65; H, 3.14; N, 3.97. Found: C, 39.49; H, 3.06; N, 4.02.

Synthesis of $Ba[H_2bpye]_2[Fe(ox)_3]_2\cdot(dmn)\cdot 3H_2O$(4). Twenty milliliters of aqueous solutions of $K_3[Fe(ox)_3]\cdot 3H_2O$ (0.82 mmol) and $H_2bpyeCl_2$ (0.8 mmol) were mixed with 5 mL of methanol solutions of 1,6-dimethoxynaphthalene (dmn) (1.5 mmol) and $BaCl_2$ (1.0 mmol) and were then left undisturbed at room temperature to allow for slow evaporation. Dark-red, block-shaped crystals of **4** were obtained in 10 days. Yield = 55%. IR (cm^{-1}): 1650, 1706, $\nu_{C=O}$, oxalate; 1221,ν_{C-O}, dmn; 1502, $\nu_{C=N}$,1396, 1624, $\nu_{C=C}$, 3454, ν_{N-H}, H_2bpye. Anal. Calcd for $C_{192}H_{176}N_{16}O_{116}Fe_8Ba_4$: C, 41.48; H, 3.09; N, 4.03. Found: C, 39.76; H, 2.87; N, 4.04.

Synthesis of $Ba[H_2bpye]_2[Fe(ox)_3]_2\cdot(dhn)\cdot 6H_2O$(5). Twenty milliliters of aqueous solutions of $K_3[Fe(ox)_3]\cdot 3H_2O$ (0.82 mmol) and $H_2bpyeCl_2$ (0.8 mmol) were mixed with 5 mL of methanol solutions of 1,5-dihydroxynaphthalene (dhn) (1.5 mmol) and $BaCl_2$ (1.0 mmol) and were then left undisturbed at room temperature to allow for slow evaporation. Dark-red, block-shaped crystals of **5** were obtained in 10 days as a single phase. Yield = 90%. IR (cm^{-1}): 1706, 1651, $\nu_{C=O}$, oxalate; 1278, ν_{C-O}, dhn; 1525, $\nu_{C=N}$, 1589, 1382, $\nu_{C=C}$, 3504, ν_{N-H}, H_2bpye. Anal. Calcd for $C_{184}H_{176}N_{16}O_{128}Fe_8Ba_4$: C, 39.08; H, 3.14; N, 3.96. Found: C, 39.49; H, 3.64; N, 4.02.

Synthesis of $[H_2bpy]_3[Fe(ox)_3]_2\cdot 3(mp)\cdot 3H_2O\cdot MeOH$ (6). Twenty milliliters of aqueous solutions of $K_3[Fe(ox)_3]\cdot 3H_2O$ (0.42 mmol) and 4,4′-bipyridinium dichloride (0.6 mmol) were mixed with 5 mL of methanol solution of 4-methoxyphenol (1.0 mmol) and were then left undisturbed at room temperature to allow for slow evaporation. Red, block-shaped crystals of **6** were obtained in 10 days. Yield = 70%. IR (cm^{-1}): 1660, 1702, $\nu_{C=O}$, oxalate; 1228,ν_{C-O}, mp; 1645, 1382, $\nu_{C=C}$, 1508, $\nu_{C=N}$, 3272, ν_{N-H}, H_2bpy. Anal. Calcd for $C_{127}H_{124}N_{12}O_{67}Fe_4$: C, 48.99; H, 4.01; N, 5.40. Found: C, 45.36; H, 3.01; N, 5.43.

Structure Determination. Single crystal X-ray diffraction data sets were collected on a Bruker APEX-II diffractometer with a CCD area detector at 120 K (Mo Kα, λ = 0.710 73 Å). The crystals were taken from the mother liquid, dried in air, and covered with Paratone-N oil before inserting them in the cold stream. The structures were solved by direct methods and refined by full-matrix least-squares based on F^2 using the SHELXL 97 program.[10] All hydrogen atoms of the framework were refined as riding on the corresponding non-hydrogen atoms, while they were omitted for some disordered and solvent molecules. One of the two crystallographically independent organic linkers in **1** was refined as disordered equally among two sites in a slip fashion along with water molecules. Similarly, some of the linkers in **5** show disorder among two positions with 82 and 18% occupancies. Compound **2** exhibits a dinuclear formation $[Fe_2(ox)_5]^{4-}$, where two $Fe(ox)_2$ parts are bridged by the fifth oxalate. Such formations with bridging bis(bidentate) oxalates are well-known not only for iron[11] but for a number of other transition metals.[12] This dinuclear complex is refined with 12% occupancy and replaces two mononuclear $[Fe(ox)_3]^{3-}$ complexes that are positioned well apart from each other and are separated by a water molecule. This disorder causes disorder in one of the two independent linkers in the structure, which takes a minor position with the same 12% occupancy. Some of the guest molecules in the compounds are disordered as well. The 4-methoxyphenol in **3** shows some disorder, where some of the molecules are rotated at 180° and others have methoxy−hydroxy positional disorder. The 1,6-dimethoxynaphthalene in **4** is disordered with 50% occupancy. In the structure **6**, one guest 4-methoxyphenol molecule was disordered with a 63:37 ratio.

Magnetic Measurements. The magnetic susceptibilities of pure polycrystalline samples were measured in the temperature range 10−300 K on a Quantum Design MPMS SQUID instrument. The data were corrected for the diamagnetism of the sample holders and the constituent atoms.

RESULTS AND DISCUSSION

The crystal structures of the guest-free frameworks **1** and **2** are topologically similar (Figure 1, Table 1). In both, the $[Fe(ox)_3]^{3-}$ anions are isolated from each other unlike the previously reported frameworks with $[Co(en)(ox)_2]^-$, which exhibit intercomplex hydrogen bonds involving the oxalate and ethylenediamine ligands.[8] Instead, in **1** and **2** water molecules positioned between the complexes perform this role as hydrogen-bonded bridges between complexes. The structures can be described as infinite hydrogen-bonded chains of $-H_2bpy-Fe(ox)_3-H_2bpy-$ with each iron complex using two of its oxalates. Pairs of chains are then interconnected by water molecules that are hydrogen-bonded to the third oxalate ligands of two metal complexes from different chains thus

dx.doi.org/10.1021/cg300293j | Cryst. Growth Des. 2012, 12, 2684−2690

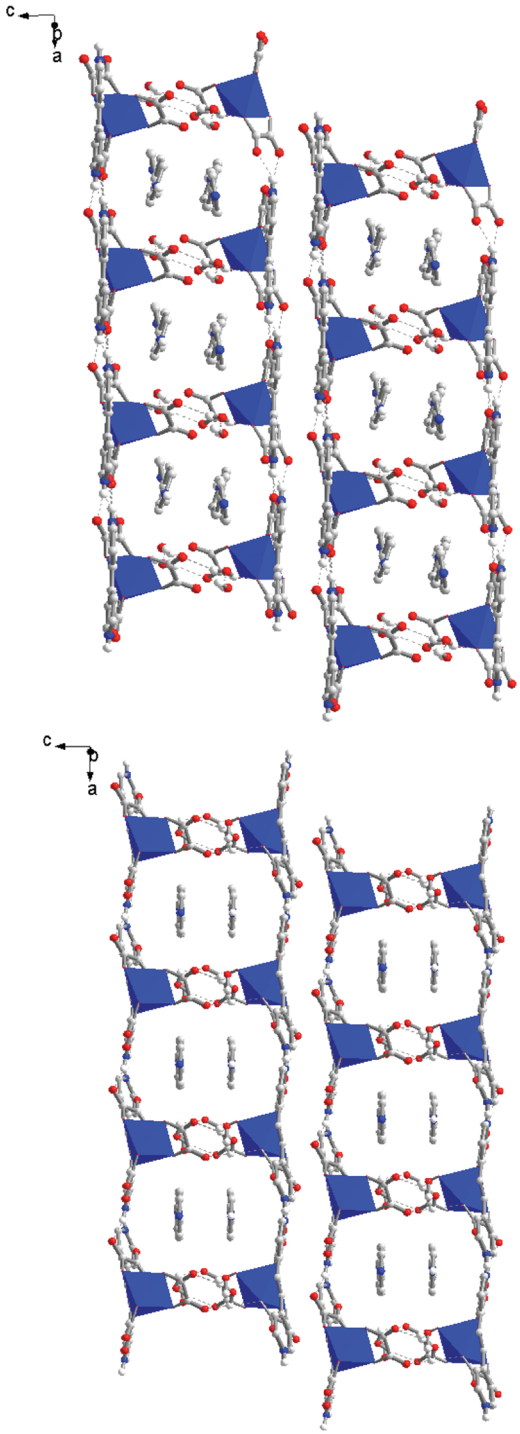

Figure 1. The ladderlike structures of **1** (top) and **2** (bottom) made of diprotonated bipyridinium linkers hydrogen-bonded (broken cyan lines) to pairs of oxalate ligands from the $[Fe(ox)_3]^{3-}$ complexes. The third oxalate ligands form the rungs of the ladders by being bridged by hydrogen-bonded water molecules. The open spaces in the ladders are occupied by monoprotonated Hbpy and Hbpye, which play the role of guest molecules.

forming ladderlike structures (Figure 1). The hydrogen bonds between the pyridyl nitrogen and the oxalate oxygen atoms are very short and in the range 2.702(5)−2.985(6) Å (Table S1 in Supporting Information). This range is very close to the previously reported distances in similar compounds.[8] The hydrogen bonds between the third oxalate and the water molecules [2.867(3)−3.053(12) Å] are somewhat longer. The spaces in the ladders openings are occupied by pairs of monoprotonated bipyridinium molecules, Hbpy or Hbpye, that are not hydrogen-bonded to the ladders (Figure 1). Instead, they exhibit $\pi-\pi$ interactions between themselves at distances of 3.316−3.637 Å (plane-to-plane) that are close to the reported literature values.[13] Not being part of the hydrogen-bonded framework and only interacting via their π systems with the linkers are typical properties of guest molecules, and therefore, these monoprotonated bipyridinium molecules can be viewed as guests in the frameworks built of their diprotonated versions H_2bpy and H_2bpye. In a way, the two structures can be viewed as self-included frameworks where one and the same organic moiety plays the role of a guest and a host.

The guest-included frameworks **3**−**5** are made of H_2bpye linkers, $[Fe(ox)_3]^{3-}$ complexes, and Ba^{2+} cations (Figures 2−4). The cations are found coordinated by four chelating oxalate ligands from four different metal complexes. In turn, each metal complex in **3** and **4** interacts with two cations, giving a ratio of 1:2 for Ba^{2+}:$[Fe(ox)_3]^{3-}$. In **5**, this same ratio is achieved by having half of the complexes bonded to three Ba^{2+} cations while the other half interacts with only one. In both cases the interactions result in extended structures. The presence of the Ba cations in that particular ratio effectively reduces the negative charge of the metal complex by one. This leads to the need of fewer cationic linkers per node for charge balancing (1 instead of 1.5) which, together with the small size of the barium, leaves more space for guest molecules.

Structurally, compounds **3** and **4** are very similar. Both exhibit chains of $(-\{Ba^{2+}\}\{[Fe(ox)_3]^{3-}\}_2\{Ba^{2+}\}-)_\infty$, where pairs of metal complexes bridge between pairs of Ba cations, thus forming infinite chains (Figures 2 and 3). Each of the two bridging metal complexes uses two of its oxalates to chelate the two barium cations while the remaining third oxalate hydrogen bonds with both oxygen atoms to a H_2bpye linker, one on each side of the chain [H-bond distances in the range 2.692(5)−3.031(5) Å]. The other end of the linker is also hydrogen bonded but to an oxalate from a neighboring chain [H-bond distances 3.231(5)−3.300(5) Å]. This results in a two-dimensional layer with overall stoichiometry $\{(H_2bpye)_2\}^{4+}\{[Fe(ox)_3]_2[Ba]\}^{4-}$. The layer has large openings between the H_2bpye the size of which is defined by both the length of the pillar and the distance between the pillars. The latter is fairly large because it is in turn defined by the size of the metal complex and the barium cations between them. The spaces between the pillars are taken by the guest molecules, one per two pillars. In addition, the smaller mp guest in **3** is found also in the interlayer spaces, a half a molecule per two pillars. This is reflected in the formulas of **3** and **4**, $Ba[H_2bpye]_2[Fe(ox)_3]_2\cdot 1.5(mp)\cdot 4.5H_2O$ and $Ba[H_2bpye]_2[Fe(ox)_3]_2\cdot(dmn)\cdot 3H_2O$, respectively. In both structures the guest molecules exhibit $\pi-\pi$ interactions with the pillars with plane-to-plane distances in the range 3.028−3.375 Å, which is consistent with previously reported values.[8] Also there are $\pi-\pi$ interactions observed between the pillars in **3** and **4** in the range of 3.443−3.5 Å. The space occupied by the guests and the solvent water molecules in the two structures is close to 26%.[14]

Compound **5** (Figure 4), as already mentioned, has the same coordination for the Ba cations, i.e., four chelating oxalate ligands from four different metal complexes per cation, but the metal complexes differ in the number of cations they are coordinated to. Half of the metal complexes use all three oxalate ligands to coordinate to three Ba-cations, while the

dx.doi.org/10.1021/cg300293j | Cryst. Growth Des. 2012, 12, 2684−2690

Table 1. Selected Data Collection and Refinement Parameters for Compounds 1−6

compound	**1** [Fe(ox)$_3$-bpy]	**2** [Fe(ox)$_3$-bpye])	**3** [Fe(ox)$_3$-bpye-mp]	**4** [Fe(ox)$_3$-bpye-dmn]	**5** [Fe(ox)$_3$-bpye-dhn]	**6** [Fe(ox)$_3$-bpy-mp]
formula	$C_{52}H_{48}N_8O_{29}$ Fe_2	$C_{59.77}H_{54}N_8O_{27.54}Fe_2$	$C_{372.8}H_{352}N_{32}O_{251.2}Fe_{16}Ba_8$	$C_{192}H_{176}N_{16}O_{116}Fe_8Ba_4$	$C_{184}H_{176}N_{16}O_{128}Fe_8Ba_4$	$C_{127}H_{124}N_{12}O_{67}Fe_4$
mw (g·mol^{-1})	1360.68	1436.69	11291.98	5559.65	5655.57	3113.78
space group, Z	$P\bar{1}$, 2	$P\bar{1}$, 2	$P2_1/n$, 8	$C2/c$, 8	$P2_1/c$, 4	$P2_1$, 4
a (Å)	10.1969(1)	9.9383(15)	10.1267(3)	10.1158(12)	25.8392(18)	9.8454(17)
b (Å)	11.0817(11)	11.9425(18)	41.4321(12)	20.723(3)	10.6613(7)	32.640(6)
c (Å)	13.9784(15)	13.6747(2)	24.9603(7)	25.027(3)	20.8311(14)	11.319(2)
α (deg)	95.445(2)	101.756(3)	90	90	90	90
β (deg)	105.167(2)	101.914(3)	92.417(1)	92.667(2)	112.231(2)	111.469(4)
γ (deg)	113.937(2)	101.952(3)	90	90	90	90
V (Å^3)	1356.7(2)	1501.24(4)	10463.29(16)	5240.6(11)	5312.0(6)	3385.0(11)
radiation, λ (Å)	Mo Kα, 0.71073					
ρ_{calcd} (g·cm^{-3})	1.665	1.589	1.792	1.762	1.768	1.527
μ (mm^{-1})	0.64	0.58	1.40	1.39	1.38	0.53
R1/*w*R2,[a] $I \geq 2\sigma_I$	0.0377, 0.0838	0.0535, 0.1299	0.0475, 0.1235	0.0525, 0.1204	0.0348, 0.0885	0.0801, 0.1704
R1/*w*R2,[a] all data	0.0581, 0.0930	0.0669, 0.1388	0.0677, 0.1369	0.0740, 0.1314	0.0533, 0.1006	0.1862, 0.2219

[a] $R1 = [\sum||F_o| - |F_o||]/\sum|F_o|$; $wR2 = \{[\sum w[(F_o)^2 - (F_c)^2]^2]/[\sum w(F_o^2)^2)]\}^{1/2}$; $w = [\sigma^2(F_o)^2 + (AP)^2 + BP]^{-1}$, where $P = [(F_o)^2 + 2(F_c)^2]/3$. Mo K$\alpha$, 0.710 73

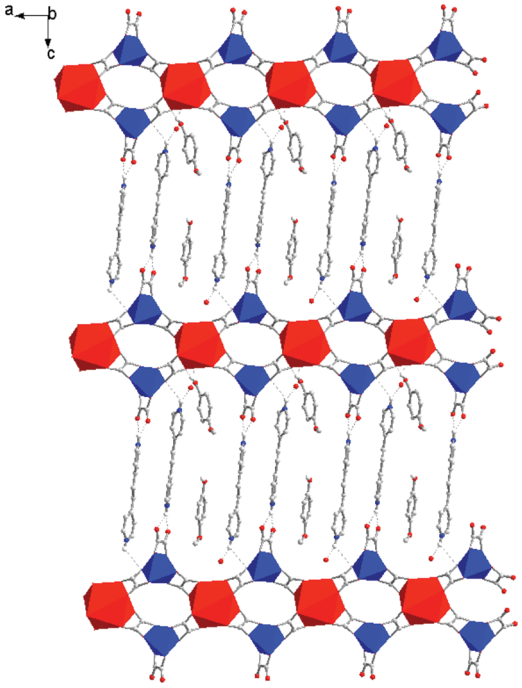

Figure 2. The structure of $Ba[H_2bpye]_2[Fe(ox)_3]_2·1.5(mp)·4.5H_2O$ (**3**) viewed along the *b*-axis (blue and red polyhedra are used for the Fe and Ba coordination spheres). Flat chains of $(-\{Ba^{2+}\}\{[Fe(ox)_3]^{3-}\}_2\{Ba^{2+}\}-)_\infty$ are linked by hydrogen-bonded H_2bpye molecules (broken lines) to form sheets with cavities occupied by the guest molecules.

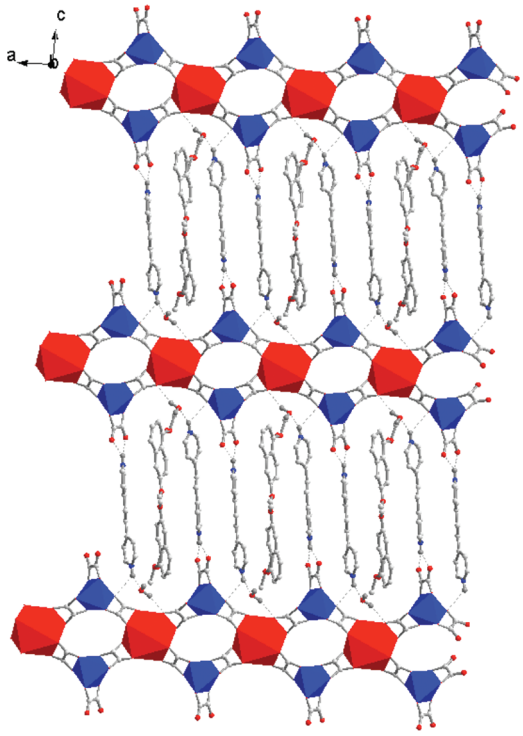

Figure 3. The structure of $Ba[H_2bpye]_2[Fe(ox)_3]_2·(dmn)·3H_2O$ (**4**) viewed along the *b*-axis (blue and red polyhedra are used for the Fe and Ba coordination spheres). The same flat chains as in **3** are linked by hydrogen-bonded H_2bpye molecules (broken lines) to form sheets with cavities occupied by the guest molecules.

other half are terminal and coordinate to only one such cation (Figure 4a). This results in wider ribbons compared to the chains in **3** and **4**. The ribbons are stacked flat but shifted on top of each other (Figure 4b), and the stacks are lined up next to each other. Half of the H_2bpye molecules play the role of linkers and connect between a ribbon of one stack and a ribbon that is two levels down in a neighboring stack (Figure 4c). This is possible because these linkers can pass through the large side openings, or bays, of the ribbons at the level in between. One side of the linkers hydrogen bonds to terminal oxalates while the other end hydrogen bonds to oxygen atoms from internal oxalates [distances of 2.779(5)−3.077(5) Å]. The other half of the H_2bpye molecules are hydrogen bonded only at one end and are thus terminal to the framework. They can be viewed as guest molecules that together with the dhn guests fill the galleries between the true linkers. All H_2bpye molecules are parallel to each other as well as to the dhn guest molecules and exhibit $\pi-\pi$ interactions in the range of 3.028−3.367 Å.

Lastly, compound **6** is a guest-included framework made of $[Fe(ox)_3]^{3-}$ and the shorter H_2bpy linkers with mp molecules as guests (Figure 5). The absence of charge-reducing Ba cations in this case results in the need for more positively charged dicationic H_2bpy linkers and thus a higher linker-to-node ratio

dx.doi.org/10.1021/cg300293j | *Cryst. Growth Des.* 2012, 12, 2684−2690

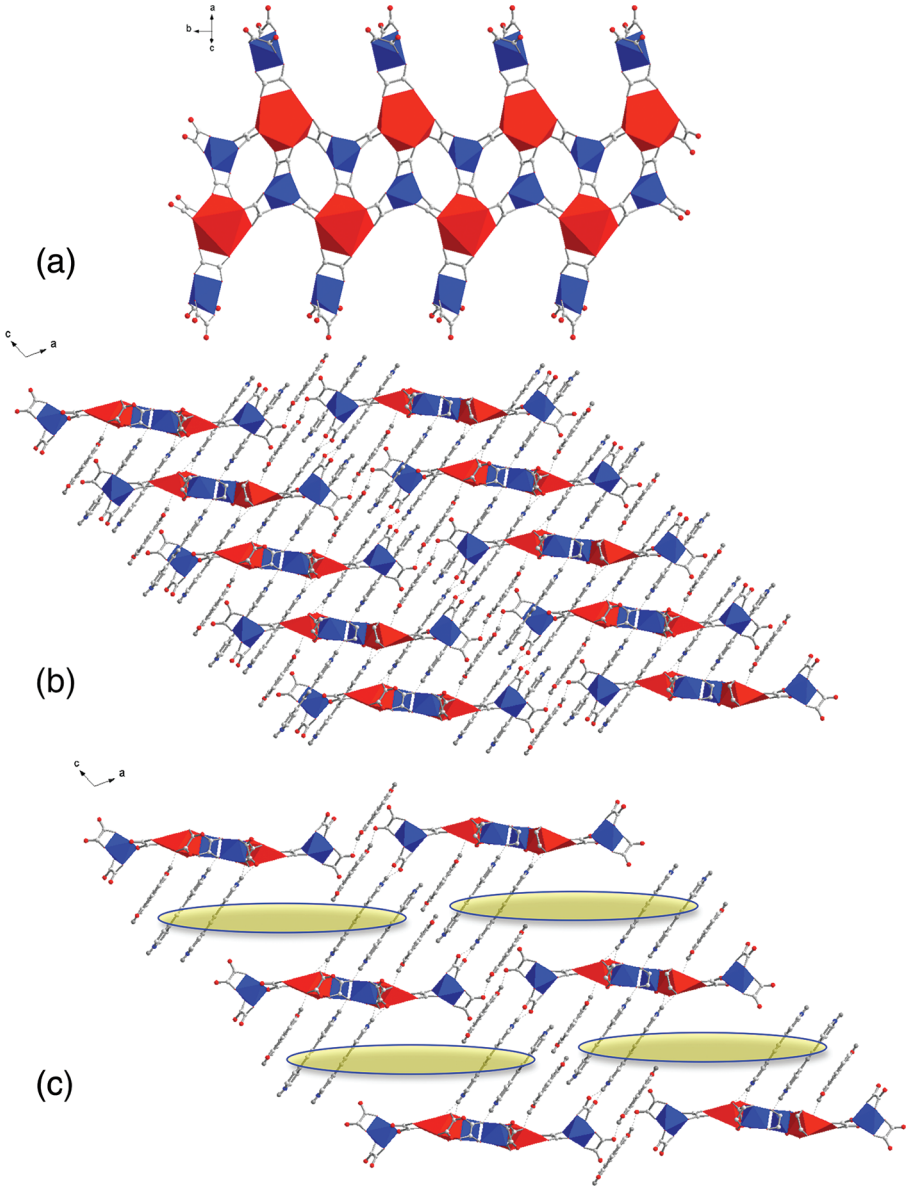

Figure 4. Two views of the structure of $Ba[H_2bpye]_2[Fe(ox)_3]_2\cdot(dhn)\cdot 6H_2O$ (**5**) showing (a) the ribbons of $\{[Fe(ox)_3]_2[Ba]\}^{4-}$ and (b and c) how they are stacked and hydrogen-bonded to H_2bpye linkers (views along the *b*-axis). In part c every other ribbon in a stack is omitted (marked with semitransparent yellow ellipses) for clearer view of the hydrogen-bonding pattern.

of 1.5 reflected in the stoichiometry $[H_2bpy]_3[Fe(ox)_3]_2\cdot 3(mp)\cdot 3H_2O\cdot MeOH$. This structure exhibits extensive hydrogen bonding not only between pillars and metal complexes [2.664(10)−2.972(12) Å] but also between the phenol proton of the mp guest and the metal complexes [2.636(16)−2.776(10) Å]. The latter interaction, however, is not a part of the framework, as the guest does not interconnect between any fragments of the framework but only acts as a pendant. In addition to this interaction, the guest exhibits additional $\pi-\pi$ interactions with the linkers, with interplanar distances in the range 3.387−3.403 Å. The best way to view this framework is as made of hydrogen-bonded chains of $[Fe(ox)_3]^{3-}$ and H_2bpy^{2+} that are, in turn, interconnected by another set of H_2bpy^{2+} linkers forming slabs of pairs of chains. The slabs are not interconnected at all, making the structure truly two-dimensional.

The presence of extensive $\pi-\pi$ interactions between the aromatic guest molecules and the linkers in the guest-inclusion compounds is clearly indicated by the color change from light-green for the guest-free frameworks to red and dark-red in the guest-included structures. This was confirmed by the UV−vis absorption spectra of the compounds and the free guest molecules, which showed an additional broad absorption in the area of 500−550 nm for the guest-inclusion compounds (Figures S1−S4 in Supporting Information). Such broad absorption bands are typical for aromatic stacks with $\pi-\pi$ interactions.[15]

The temperature dependence of the magnetizations of the six compounds showed the expected paramagnetic behavior (Figures S5−S10 in Supporting Information). The iron complexes in all behave as isolated magnetic centers in magnetically dilute systems. The effective magnetic moments μ_{eff} of compounds **1**−**5** are in the range of 5.4−6.0 expected for weak field Fe^{3+} ions with five unpaired electrons. The plots of the temperature dependence of the inverse magnetic susceptibilities are nearly perfectly straight lines following the Curie law. Only compound **6** showed deviation from this at

dx.doi.org/10.1021/cg300293j | *Cryst. Growth Des.* 2012, 12, 2684−2690

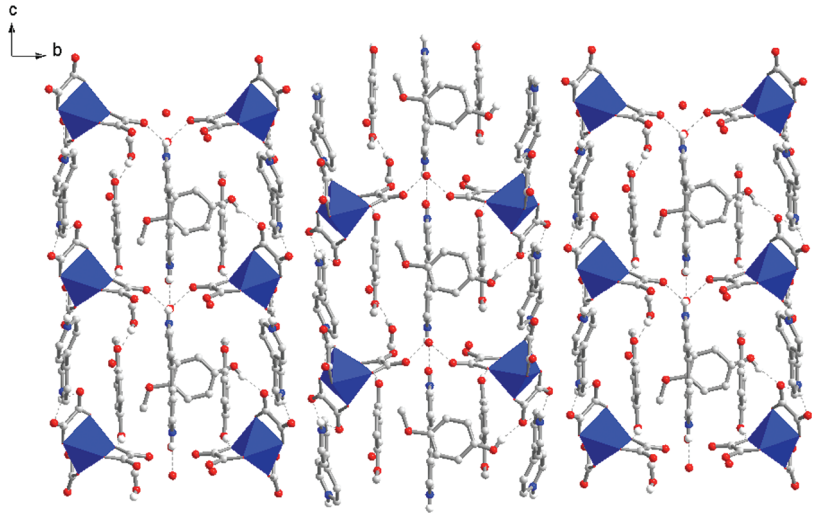

Figure 5. The structure of compound $[H_2bpy]_3[Fe(ox)_3]_2{\cdot}3(mp){\cdot}3H_2O{\cdot}MeOH$ (**6**). View along *a*-axis, showing the packing of the $[Fe(ox)_3]^{-3}$ metal complexes with H_2bpy linkers with hydrogen-bonding interactions (broken cyan lines) along with guest mp and solvent water molecules.

low temperatures, indicating possible antiferromagnetic interactions. This is also in agreement with the negative Weiss temperature for the higher temperature straight line fit with the Curie–Weiss law. However, on the basis of the structure, it is impossible to imagine any interactions between the iron centers being so far apart (7.911 Å). It is more likely that a small amount of antiferromagnetic Fe-based impurity is present in the sample and influences the measurements.

To recap, the newly synthesized two guest-free and four guest-inclusion frameworks demonstrate again the structural versatility and apparent abundance of compounds based on charge-assisted hydrogen bonds between anionic metal complexes and cationic organic linkers. They also demonstrate the usefulness of small ions for reducing the high charges of the oppositely charged metal complexes and thus reducing the number of organic linkers per complex. This, in turn, leaves more space for guest molecules to take in the guest-included structures. As in previous cases, a substantial part of the driving force for the insertion of aromatic guest molecules in the frameworks comes from their $\pi-\pi$ interactions with the aromatic organic linkers.

■ ASSOCIATED CONTENT

Supporting Information

X-ray crystallographic files in CIF format, UV–vis spectra, magnetic moment and inverse magnetic susceptibility plots, and hydrogen-bond distances for the six compounds. This material is available free of charge via the Internet at http://pubs.acs.org.

■ AUTHOR INFORMATION

Corresponding Author

*E-mail: ssevov@nd.edu.

Notes

The authors declare no competing financial interest.

■ ACKNOWLEDGMENTS

We thank the National Science Foundation for the financial support (DMR-0968645) and the Materials Characterization Facility at the center for Sustainable Energy at Notre Dame (cSEND) for the UV–vis measurements.

■ REFERENCES

(1) Holman, K. T.; Pivovar, A. M.; Swift, J. A.; Ward, M. D. *Acc. Chem. Res.* **2001**, *34*, 107–108.

(2) (a) MacNicol, D. D., Toda, F., Bishop, R., Eds. *Comprehensive Supramolecular Chemistry, Vol. 6: Solid-State Supramolecular Chemistry, Crystal Engineering*; Pergamon Press: Oxford, 1996. (b) Nassimbeni, L. R. *Acc. Chem. Res.* **2003**, *36*, 631–637. (c) Kim, J.; Lee, S. O.; Yi, J.; Kim, W. S.; Ward, M. D. *Sep. Purif. Technol.* **2008**, *62*, 517–522. (d) Kim, J.; Yi, J.; Ward, M. D.; Kim, W. S. *Sep. Purif. Technol.* **2009**, *66*, 57–64.

(3) (a) Ward, M. D. *Chem. Commun.* **2005**, 5838–5842. (b) Melendez, R. E.; Sharma, C. V. K.; Zaworotko, M. J.; Bauer, C.; Rogers, R. D. *Angew. Chem., Int. Ed.* **1996**, *35*, 2213–2215. (c) Biradha, K.; Dennis, D.; MacKinnon, V. A.; Sharma, K. C. V.; Zaworotko, M. J. *J. Am. Chem. Soc.* **1998**, *120*, 11894–11903. (d) Hosseini, M. W. *Acc. Chem. Res.* **2005**, *38*, 313–323. (e) Dechambenoit, P.; Ferlay, S.; Kyritsakas, N.; Hosseini, M. W. *Chem. Commun.* **2009**, 1559–1561.

(4) (a) Holman, K. T.; Ward, M. D. *Angew. Chem., Int. Ed.* **2000**, *39*, 1653–1656. (b) Custelcean, R.; Ward, M. D. *Cryst. Growth Des.* **2005**, *5*, 2277–2287. (c) Russell, V. A.; Etter, M. C.; Ward, M. D. *Chem. Mater.* **1994**, *6*, 1206–1217. (d) Swift, J. A.; Reynolds, A. M.; Ward, M. D. *Chem. Mater.* **1998**, *10*, 4159–4186. (e) Pivovar, A. M.; Holman, K. T.; Ward, M. D. *Chem. Mater.* **2001**, *13*, 3018–3031. (f) Pivovar, A. M.; Ward, M. D.; Brown, C. M.; Neumann, D. A. *J. Phys. Chem. B.* **2002**, *106*, 4916–4924. (g) Holman, K. T.; Martin, S. M.; Parker, D. P.; Ward, M. D. *J. Am. Chem. Soc.* **2001**, *123*, 4421–4431. (h) Holman, K. T.; Pivovar, A. M.; Ward, M. D. *Science* **2001**, *294*, 1907–1911. (i) Russell, V. A.; Evans, C. C.; Li, W. J.; Ward, M. D. *Science* **1997**, *276*, 575–579. (j) Ward, M. D. *Struct. Bonding (Berlin)* **2009**, *132*, 1–23. (k) Soegiarto, A. C.; Ward, M. D. *Cryst. Growth Des.* **2009**, *9*, 3803–3815. (l) Soegiarto, A. C.; Comotti, A.; Ward, M. D. *J. Am. Chem. Soc.* **2010**, *132*, 14603–14616.

(5) (a) Wang, X. Y.; Sevov, S. C. *Chem. Mater.* **2007**, *19*, 4906–4912. (b) Wang, X. Y.; Sevov, S. C. *Cryst. Growth Des.* **2008**, *8*, 1265–1270. (c) Wang, X. Y.; Justice, R.; Sevov, S. C. *Inorg. Chem.* **2007**, *46*, 4626–4631. (d) Dalrymple, S. A.; Shimizu, G. K. H. *J. Am. Chem. Soc.* **2007**, *129*, 12114–12116. (e) Darlrymple, S. A.; Shimizu, G. K. H. *Chem. Commun.* **2006**, 956–958. (f) Sharma, R. P.; Bala, R.; Sharma, R. *Acta Crystallogr.* **2006**, *E62*, m2113–m2115. (g) Darlrymple, S. A.; Shimizu, G. K. H. *J. Mol. Struct.* **2006**, *796*, 95–106. (h) Dalrymple, S. A.; Parvez, M.; Shimizu, G. K. H. *Chem. Commun.* **2001**, 2672–2673. (i) Darlrymple, S. A.; Parvez, M.; Shimizu, G. K. H. *Inorg. Chem.* **2002**, *41*, 6986–6996. (j) Côté, A. P.; Shimizu, G. K. H. *Chem.—Eur. J.* **2003**, *9*, 5361–5370. (j) Zhou, J. S.; Cai, J. W.; Ng, S. W. *Acta Crystallogr.* **2003**, *E59*, o1185–o1186. (k) Cai, J. W.; Hu, X. P.; Yao, J. H.; Ji, L. N. *Inorg. Chem. Commun.* **2001**, *4*, 478–482. (l) Cai, J. W.;

Feng, X. L.; Hu, X. P. *Acta Crystallogr.* **2001**, *C57*, 1168−1170. (m) Chen, C. H.; Cai, J. W.; Chen, X. M. *Acta Crystallogr.* **2002**, *C58*, m59−m60. (n) Chen, C. H.; Cai, J. W.; Feng, X. L.; Chen., X. M. *J. Chem. Cryst.* **2002**, *31*, 271−280. (o) Huo, L. H.; Gao, S.; Lu, Z. Z.; Xu, S. X.; Zhao, H. *Acta Crystallogr.* **2004**, *E60*, m1205−m1207.

(6) Reddy, D. S.; Duncan, S.; Shimizu, G. K. H. *Angew. Chem., Int. Ed.* **2003**, *42*, 1360−1363.

(7) (a) Mouchaham, G.; Roques, N.; Imaz, I.; Duhayon, C.; Sutter, J. P. *Cryst. Growth Des.* **2010**, *10*, 4906−4919. (b) Mouchaham, G.; Roques, N.; Kaiba, A.; Guionneauc, P.; Sutter, J. P. *CrystEngComm* **2010**, *12*, 3496−3498. (c) Thétiot, F.; Duhayon, C.; Venkatakrishnan, T. S.; Sutter, J. P. *Cryst. Growth Des.* **2008**, *8*, 1870−1877. (d) Imaz, I.; Thillet, A.; Sutter, J. P. *Cryst. Growth Des.* **2007**, *7*, 1753−1761. (e) Atencio, R.; Bricen, A.; Silva, P.; Rodríguez, J. A.; Hanson, J. C. *New J. Chem.* **2007**, *31*, 33−38. (f) Atencio, R.; Briceno, A.; Galindo, X. *Chem. Commun* **2005**, 637−639. (g) Han, Z.; Gao, Y.; Zhai, X.; Peng, J.; Tian, A.; Zhao, Y.; Hu, C. *Cryst. Growth Des.* **2009**, *9*, 1225−1234.

(8) Prakash, M. J.; Sevov, S. C. *Inorg. Chem.* **2011**, *50*, 12739−12746.

(9) Booth, H. S. *Inorganic Synthesis*; McGraw-Hill Book Company, Inc.: New York, 1939; Vol. *1*, pp 36.

(10) *SHELXTL version 5.1*; Bruker Analytical Systems: Madison, WI, 1997.

(11) (a) Armentano, D.; Munno, G. D.; Lloret, F.; Julve, M. *CrystEngComm* **2005**, *7*, 57−66. (b) Coronado, E.; Galán-Mascarós, J. R.; Gómez-García, C. J. *J. Chem. Soc., Dalton Trans.* **2000**, 205−210.

(12) (a) Triki, S.; Bérézovsky, F.; Pala, J. S.; Gómez-García, C. J.; Coronado, E.; Costuas, K.; Halet, J. F. *Inorg. Chem.* **2001**, *40*, 5127−5132. (b) Masters, V. M.; Sharrad, C. A.; Bernhardt, P. V.; Gahan, L. R.; Moubaraki, B.; Murray, K. S. *J. Chem. Soc., Dalton Trans.* **1998**, 413−416. (c) Fuller, A. L.; Watkins, R. W.; Dunbar, K. R.; Prosvirin, A. V.; Arif, A. M.; Berreau, L. M. *J. Chem. Soc., Dalton Trans.* **2005**, 1891. (d) Zhu, L. H.; Zeng, M. H.; Ng, S. W. *Acta Crystallogr.* **2005**, *E61*, m916−m918. (e) Shi, C.; Fan, L.; Wei, P.; Li, B.; Zhanga, X. *Acta Crystallogr.* **2010**, *E66*, m822. (f) Yang, X.; Li, J.; Wang, H. W.; Zhao, X. H.; Shan, Y. K. *Acta Crystallogr.* **2007**, *E63*, m1554. (g) Román, P.; Guzmán-Miralles, C.; Luque, A.; Beitia, J. I.; Cano, J.; Lloret, F.; Julve, M.; Alvarez, S. *Inorg. Chem.* **1996**, *35*, 3741−3751. (h) Zheng, A. L.; Ju, Z. F.; Li, W.; Zhang, J. *Inorg. Chem. Commun.* **2006**, *9*, 489−492. (i) Qian, J.; Wang, L.; Gu, W.; Liu, X.; Tian, J.; Yan, S. *J. Chem. Soc., Dalton Trans.* **2011**, *40*, 5617. (j) Vaidhyanathan, R.; Natarajan, S.; Rao, C. N. R. *J. Chem. Soc., Dalton Trans.* **2001**, 699−706.

(13) (a) Kawase, T.; Kurata, H. *Chem. Rev.* **2006**, *106*, 5250−5273. (b) Hunter, C. A.; Sanders, J. K. M. *J. Am. Chem. Soc.* **1990**, *112*, 5525−5534. (c) Muehldorf, A. V.; Engen, D. V.; Warner, J. C.; Hamilton, A. D. *J. Am. Chem. Soc.* **1988**, *110*, 6561−6562.

(14) Spek, A. L. *PLATON, a Multipurpose Crystallographic Tool*; Utrecht University: Utrecht, The Netherlands, 2007.

(15) (a) Liu, Y.; Bruneau, A.; He, J.; Abliz, Z. *Org. Lett.* **2008**, *10*, 765−768. (b) Liu, M.; Li, S.; Zhang, M.; Zhou, Q.; Wang, F.; Hu, M.; Fronczek, F. R.; Li, N.; Huang, F. *Org. Biomol. Chem.* **2009**, *7*, 1288−1291.